Available online at www.sciencedirect.com
SCIENCE DIRECT®
PHYSICS LETTERS B
ELSEVIER
Physics Letters B 554 (2003) 115–120
www.elsevier.com/locate/npe

Signature inversion caused by shape change in ^{84}Rb

Shuifa Shen [a,b], Jiahui Gu [a], Shuanghui Shi [a], Jingyi Liu [a], Jianzhong Zhou [a], Wenqing Shen [a]

[a] *Shanghai Institute of Nuclear Research, The Chinese Academy of Sciences, Shanghai 201800, PR China* [1]
[b] *CCAST (World Lab.), P.O. Box 8730, Beijing 100080, PR China*

Received 6 February 2002; received in revised form 12 September 2002; accepted 30 December 2002

Editor: W. Haxton

Abstract

The angular momentum projected shell model (PSM) is applied to the nucleus ^{84}Rb. The results of theoretical calculations about the positive-parity yrast band with configuration $\pi g_{9/2} \otimes \nu g_{9/2}$ and the negative-parity yrast band with configuration $\pi(p_{3/2}, f_{5/2}) \otimes \nu g_{9/2}$ are compared with experimental data. The interpretation within the projected shell model shows that the signature inversion displayed in the positive-parity yrast band in this nucleus is a signal of a substantial quadrupole shape change with increasing spin where the nucleus evolves from a prolate shape at low spin through a triaxial shape to an oblate shape at high spin. In addition, we also specify the nuclear shape for these two bands.

PACS: 21.60.Cs; 27.50.+e; 21.10.Hw

Keywords: Projected shell model (PSM); Yrast state; Quadrupole deformation

Excited states in the double-odd nucleus ^{84}Rb have mainly been studied via the ^{81}Br$(\alpha, n)^{84}$Rb reaction by means of in-beam γ-ray spectroscopy in 1991 [1]. In that work, on top of the $5^{(+)}$ isomer a level sequence with increasing spins up to $10\hbar$ and probably positive-parity has been identified. These states are ascribed to the configuration $\pi g_{9/2} \otimes \nu g_{9/2}$. The negative-parity states in ^{84}Rb originate from the unpaired neutron occupies the almost filled $g_{9/2}$ orbit and the unpaired proton moves in the almost filled orbits $f_{5/2}$ or $p_{3/2}$.

High-spin states of the double-odd nucleus ^{86}Rb, which contains only two neutrons more than the nucleus ^{84}Rb, have been investigated via the reaction ^{82}Se$(^{7}$Li$, 3n)^{86}$Rb in 1994 [2]. The new high-spin level scheme of ^{86}Rb is interpreted on the basis of shell-model calculations in the configuration space $2p_{3/2}$, $1f_{5/2}$, $2p_{1/2}$ and $1g_{9/2}$ for the protons and $2p_{1/2}$, $1g_{9/2}$ and $2d_{5/2}$ for the neutrons. In that Letter, in agreement with the experimental result the ground state is predicted as the 2^- level which is characterized by the coupling of one neutron hole in the $1g_{9/2}$ orbital to the $\pi(1f_{5/2}^5, 2p_{3/2}^4)$ configuration. The same structure is prevailed in the wave function of the lowest 7^- level whereas the lowest 6^- state is predominantly

E-mail address: ssh@sinr.ac.cn (S. Shen).
[1] Mailing address.

0370-2693/03
doi:10.1016/S0370-2693(03)00002-9

formed by coupling one hole in the $\nu\ 1g_{9/2}$ orbital to the $\pi(1f_{5/2}^6, 2p_{3/2}^3)$ configuration.

High-spin states in adjacent odd–odd nucleus ^{82}Rb were studied through the ^{68}Zn(^{18}O, $p3n$)^{82}Rb reaction at 56 MeV beam energy via a thin target coincidence measurement [3]. Signature inversion has been seen around spin 11, somewhat shifted to the higher spins when compared with the lighter odd–odd ^{76,78}Rb isotopes, which have a signature inversion at spin 9. This shift could be a consequence of the expected decrease in quadrupole deformation (^{76,78}Rb: $\beta_2 \approx 0.38$ and ^{82}Rb: $\beta_2 \approx 0.2$) for increasing N in odd–odd Rb isotopes. In addition, for positive-parity states at low rotational frequency, i.e., at $\hbar\omega \leqslant 0.292$ MeV, the total Routhian surfaces (TRS) calculations in that work [3] predict that the nucleus ^{82}Rb is very γ soft with a quadrupole deformation of at most $\beta_2 \approx 0.23$. With increasing frequency, the nucleus becomes slightly more deformed and more stiff at an oblate shape ($\beta_2 \approx 0.25$, $\gamma = -57°$).

In the mass 80 region, the deformation depends strongly on the occupation of the proton and neutron intruder high-j $g_{9/2}$ subshells, in particular, on the low-Ω orbitals. For example, collective high-spin bands built on low-lying isomers in the nuclei ^{74,76}Br [4–6] and ^{76,78}Rb [7,8] have provided evidence for the occurrence of well-deformed nuclear shapes with a quadrupole deformation of $\beta_2 \approx 0.38$. With increasing neutron number towards the neutron shell closure at $N = 50$ this deformation-driving feature diminishes and the experimental excitation spectrum can be well explained in the framework of the spherical shell model, as demonstrated for the odd–odd nucleus ^{86}Rb [2]. So we can predict that the nucleus ^{84}Rb has a moderate deformation since for 47 neutrons the $g_{9/2}$ subshell is more than half filled and the deformation driving property of the neutron configuration is strongly reduced.

In this Letter the results of investigation about positive-parity yrast states, especially about the signature inversion in this band, and the negative-parity yrast band in ^{84}Rb in the framework of the projected shell model (PSM) are presented. Prior to the present work, there was no information available for the mechanism of signature inversion in this nucleus.

The projected shell model [9–12] employed in this Letter is a microscopic theory, which solves the many-nucleon system fully quantum mechanically. The ansatz for the angular-momentum-projected wave function is given by

$$|IM\rangle = \sum_k f_k \widehat{P}^I_{MK_k} |\varphi_k\rangle, \tag{1}$$

where k labels the basis states. $\widehat{P}^I_{MK}$ is the angular momentum projection operator which is explicitly given in Ref. [9]. Acting on an intrinsic state $|\varphi_k\rangle$, the operator $\widehat{P}^I_{MK}$ generates states of good angular momentum, thus restoring the necessary rotational symmetry violated in the deformed mean field. In this way the new shell model basis is constructed in which the Hamiltonian is diagonalized, this shell model basis taken in the present Letter is as follows:

$$\widehat{P}^I_{MK} |\varphi_k\rangle. \tag{2}$$

Actually, the basis of the projected shell model is not orthonormal. However, since the unperturbed states are degenerate, one can take an appropriate set of their linear combinations to construct an orthonormal basis. The coupling matrix elements should then be understood to be those with respect to the corresponding basis [12].

The basis states $|\varphi_k\rangle$ are spanned by the set

$$\left\{a_n^+ a_p^+ |0\rangle\right\}, \tag{3}$$

for doubly-odd nuclei. $|0\rangle$ denotes the quasiparticle vacuum state and $a_n^+(a_p^+)$ is the neutron (proton) quasiparticle creation operator for this vacuum; the index $n(p)$ runs over selected neutron (proton) quasiparticle states and k in Eq. (1) runs over the configuration of Eq. (2). The vacuum is obtained by diagonalizing a deformed Nilsson Hamiltonian [13] followed by a BCS calculation. In the calculations, we have used three major shells, i.e., $N = 2, 3$ and 4 ($N = 2, 3$ and 4) for neutrons (protons) as the configuration space.

In this Letter we have used the Hamiltonian [12]

$$\widehat{H} = \widehat{H}_0 - \frac{1}{2}\chi \sum_\mu \widehat{Q}^+_\mu \widehat{Q}_\mu - G_M \widehat{P}^+ \widehat{P} - G_Q \sum_\mu \widehat{P}^+_\mu \widehat{P}_\mu, \tag{4}$$

where $\widehat{H}_0$ is the spherical single-particle shell model Hamiltonian, $\widehat{Q}_\mu$ is the quadrupole moment operator, $\widehat{P}$ and $\widehat{P}_\mu$ are monopole pairing operator and quadrupole pairing operator, respectively. Though the

theory itself is not bound to any particular form of Hamiltonian, the advantage of using such a separable-force Hamiltonian is that the role of each interaction is well known and, therefore, the interpretation of the numerical result becomes easier. The interaction strengths are determined as follows: the strength of the quadrupole–quadrupole interaction χ is adjusted by the self-consistent relation such that the input quadrupole deformation ε_2 and the one resulting from the HFB (Hartree–Fock–Bogolyubov) procedure coincide with each other [12]. The monopole pairing strength constant is adjusted to give the known energy gap

$$G_M = \left[20.12 \mp 13.13\frac{N-Z}{A}\right] \cdot A^{-1}, \tag{5}$$

where "−" for neutrons and "+" for protons. Finally the quadrupole pairing strength G_Q is simply assumed to be proportional to G_M

$$\left(\frac{G_Q}{G_M}\right)_n = \left(\frac{G_Q}{G_M}\right)_p = \gamma. \tag{6}$$

The proportionality constant γ is chosen as 0.20 for all the bands calculated in the Letter work.

The weights f_k in Eq. (1) are determined by diagonalizing the Hamiltonian $\widehat{H}$ in the basis given by Eq. (3) as outlined in Ref. [12]. Projection of good angular momentum onto each intrinsic state generates the rotational band associated with this intrinsic configuration $|\varphi_k\rangle$. For example, $\widehat{P}^I_{MK} a_n^+ a_p^+ |0\rangle$ will produce a $2qp$ proton–neutron band. The energies of each band are given by the normalized diagonal elements according to Ref. [9]. A diagram in which $E_k(I)$ for various bands are plotted against spin I is referred to as a band diagram [12]. The lowest eigenvalue of the Hamiltonian for a given spin is named the yrast energy, and can be compared with the experiment. In this Letter, we decide to compare the experimentally observed positive-parity yrast states, especially the signature inversion in this band, and negative-parity yrast band of ^{84}Rb with the predictions of the PSM.

The projected shell model has at least two advantages by this token: (1) The procedure of angular momentum coupling, which must be done troublesomely in the conventional shell model, is done automatically by the projector irrespective of the number of quasiparticles (qp) involved. (2) It allows us to choose various multi-qp bases according to physical importance. Unfortunately, our present computer code assumes axial symmetry so that we cannot investigate those γ-deformed nuclei quantitatively [14]. The model has achieved considerable success when it was applied to the rare-earth region where the nucleus is well-deformed. In this Letter, we try to apply this model to the $A \sim 80$ region and to show the potential of this model via the study of low- and high-spin states of ^{84}Rb.

In our calculations, the following formulae are used to calculate the pairing gap parameters Δ_p and Δ_n [15]:

$$\Delta_p = \frac{1}{4}\big\{B(N,Z-2) - 3B(N,Z-1) + 3B(N,Z) - B(N,Z+1)\big\}, \tag{7}$$

$$\Delta_n = \frac{1}{4}\big\{B(N-2,Z) - 3B(N-1,Z) + 3B(N,Z) - B(N+1,Z)\big\}, \tag{8}$$

the values of the total nuclear binding energy B are taken from Ref. [16]. The results are $\Delta_p = 1.0725$ MeV and $\Delta_n = 0.9875$ MeV. The spin–orbit force parameters, κ and μ, appearing in the Nilsson potential are taken from the compilation of Zhang et al. [17] which is a modified version of Bengtsson and Ragnarsson [18] and has been fitted to the latest experimental data. It is supposed to apply over a sufficiently wide range of shells. These κ and μ are different for different major shells (N-dependent). Shape calculations using the Nilsson + BCS formalism were carried out for the nucleus ^{84}Rb, the Hartree–Fock–Bogoliubov energy E_{HFB} (approximately equivalent to the deformation energy from the calculations using the Nilsson + BCS method [12]) of ^{84}Rb as a function of quadrupole deformation ε_2 is shown in Fig. 1. It can be found that the energy E_{HFB} has two minima in Fig. 1, they correspond to the prolate shape ($\varepsilon_2 = 0.20$) and the oblate shape ($\varepsilon_2 = -0.30$), respectively, and that these two minima are considered the equilibrium deformation. It should be pointed out here that the relationship between the ε_2 and β_2 deformation parameters is as follows [19]:

$$\varepsilon_2 \approx 0.944\beta_2 - 0.122\beta_2^2 + 0.154\beta_2\beta_4 - 0.199\beta_4^2. \tag{9}$$

If the first term is adopted only, then $\varepsilon_2 = 0.20$ is approximately equivalent to $\beta_2 = 0.212$ and $\varepsilon_2 = -0.30$ is approximately equivalent to $\beta_2 = -0.318$, respectively. Therefore, we take quadrupole deformations

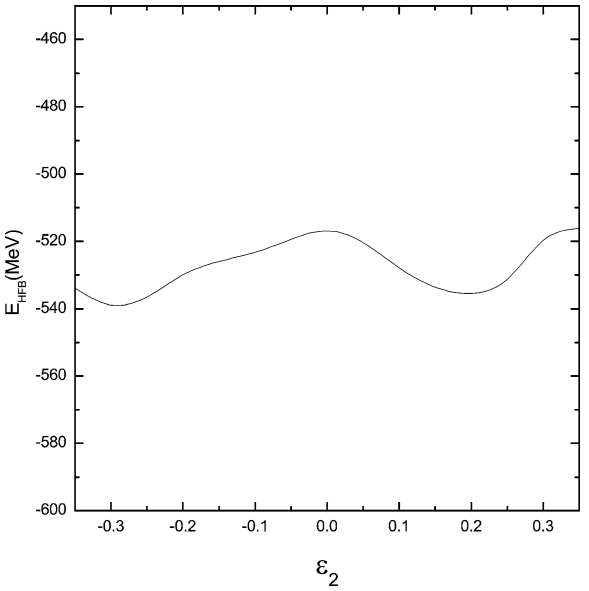

Fig. 1. Hartree–Fock–Bogoliubov energy E_{HFB} of ^{84}Rb as a function of quadrupole deformation parameter ε_2.

of $\varepsilon_2 = 0.20$ and $\varepsilon_2 = -0.30$, respectively, to calculate the positive-parity yrast states. The hexadecapole deformation parameter $\varepsilon_4 = 0.007$ is taken from the compilation of Möller et al. [16]. In the calculations, the configuration space is constructed by selecting the qp states close to the Fermi energy in the $N = 4$ ($N = 4$) major shell for neutrons (protons), i.e., $K = 1/2,\ 3/2,\ 5/2,\ 7/2$ orbitals of $g_{9/2}$ subshell (all orbitals of $g_{9/2}$ subshell) when $\varepsilon_2 = 0.20$ is adopted and $K = 1/2,\ 3/2,\ 5/2,\ 7/2$ orbitals of $g_{9/2}$ subshell ($K = 3/2,\ 5/2,\ 7/2,\ 9/2$ orbitals of $g_{9/2}$ subshell) when $\varepsilon_2 = -0.30$ is adopted, respectively, and forming multi-qp states from them. The comparison of the experimentally observed signature inversion in the positive-parity yrast levels of ^{84}Rb with the predictions of the PSM is given in Fig. 2(a) ($\varepsilon_2 = 0.20$) and Fig. 2(b) ($\varepsilon_2 = -0.30$), respectively. The experimental data have been taken from Ref. [20]. From both these figures, we cannot find signature inversion in our calculations. But if we take quadrupole deformations equal to $\varepsilon_2 = 0.20$ ($5 \leqslant I \leqslant 8$) and $\varepsilon_2 = -0.30$ ($I \geqslant 9$), respectively, to calculate the positive-parity yrast states, as shown in Fig. 2(c), the predictions for the yrast states of positive-parity are in obviously satisfactory agreement with the experiment except the energy separation between the states with $I^\pi = 10^+$

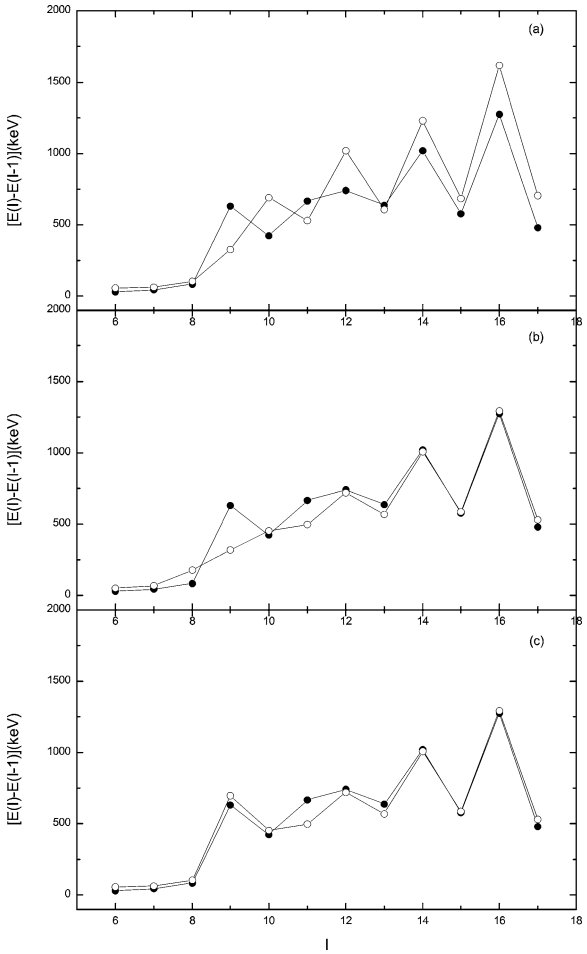

Fig. 2. The transition energies of the positive-parity yrast band in ^{84}Rb. The energy difference $E(I) - E(I-1)$ is compared between theory (open circle) and experiment (solid circle). Data are taken from Ref. [20].

and $I^\pi = 11^+$, i.e., the reproduction of this small region is not so satisfactory. This is because at this region the nucleus may be triaxial and our computer code has been written assuming an axially symmetric system, this is the best we can do at the moment [12]. But we still find that the most remarkable feature of Fig. 2(c) is that the signature inversion is reproduced at the right place. The positive-parity yrast band observed in this nucleus displays a signature inversion around spin $I = 11$. The interpretation within the projected shell model shows that this signature pattern is a signal of a substantial quadrupole shape change with increasing spin where the nucleus evolves

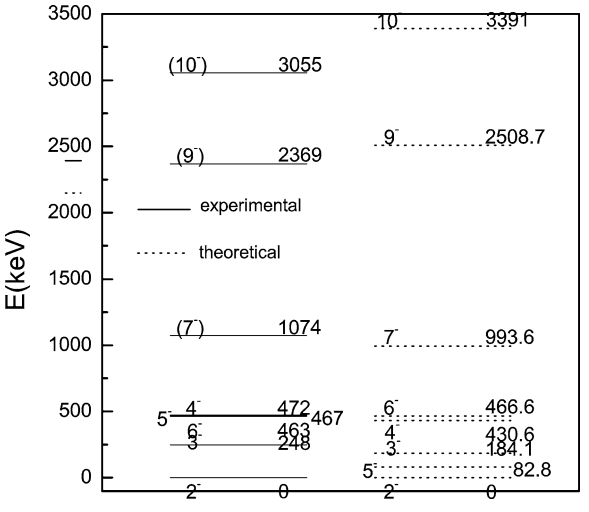

Fig. 3. Projected shell model calculations for negative-parity yrast states in ^{84}Rb compared with the experimental data.

from a prolate shape at low spin through a triaxial shape to an oblate shape at high spin. The reliability of the present conclusion is further supported by the fact that a similar shape change describes the properties of the positive-parity yrast band in the neighboring ^{82}Rb nucleus as mentioned in the introduction.

In the negative-parity ground-state band calculations, the configuration space is constructed by selecting the qp states close to the Fermi energy in the $N = 4$ ($N = 3$) major shell for neutrons (protons), i.e., $K = 7/2$ orbital of $g_{9/2}$ subshell (all orbitals of $p_{3/2}$ and $f_{5/2}$ subshells), and forming multi-qp states from them. The negative-parity yrast band, calculated also for a $\varepsilon_2 = 0.20$ deformation parameter, seems to give the best reproduction of the experiment. The theoretical energy of the negative-parity yrast band is compared with the experimental data as shown in Fig. 3. The experimental levels have been taken from Ref. [20]. In the projected shell model calculation, by taking a quadrupole deformation of $\varepsilon_2 = 0.20$ and a hexadecapole deformation of $\varepsilon_4 = 0.007$, the ground-state spin and parity of ^{84}Rb were calculated to be 2^-, which is consistent with the experimental results. The nucleus ^{84}Rb has been calculated to be almost spherical in its 2^- ground-state with a small quadrupole deformation of $\varepsilon_2 = 0.075$ (equivalent to $\beta_2 = 0.080$ [16]) when a finite-range droplet macroscopic model and a folded-Yukawa single-particle microscopic model are used [16]. But when we use this quadrupole deformation to calculate the negative-parity yrast states, the fit is rather bad for these experimental data. So in the present work the deformation of this ground-state band is tentatively assigned as $\varepsilon_2 = 0.20$.

In the ^{82}Rb nucleus, for negative-parity states at low rotational frequency, the TRS calculations [3] predict an almost spherical shape for such configurations where the valence neutron is occupying the $g_{9/2}$ subshell. This is no surprise since for 45 neutrons the $g_{9/2}$ subshell is half filled and the deformation driving property of the neutron configuration is strongly reduced. At higher frequency, e.g., at 0.487 MeV, two minima develop at a less-deformed near-prolate and a near-oblate shape. However, the near-oblate minimum disappears again with further increasing frequency. In general, the TRS calculations support the conclusion that the ^{82}Rb nucleus does not have a stable deformation at low spins. Through our present calculations, we think that the similar situation is in the ^{84}Rb.

In summary, theoretical analysis of two low-lying bands designated as positive-parity yrast band that starts from 5^+ and negative-parity yrast band that starts from 2^- is performed and compared with the experimental data, especially the signature inversion at intermediate spin around 11^+ in the positive-parity yrast band is discussed in the framework of projected shell model. It is suggested that the signature inversion in the positive-parity yrast band of ^{84}Rb may be understood in the projected shell model if the shape change taken into account, i.e., quadrupole deformation is assumed to be positive (prolate) below the inversion point ($I \sim 11$), through a triaxial shape, and to be negative (oblate) above it, the condition necessary for the signature inversion. Such a situation is reported here for the first time for $A \sim 80$ nuclei.

Acknowledgements

We are indebted to Profs. H. Hara and Y. Sun for the computer code. This work is supported by the Major State Basic Research Development Program in China under Contract No. G2000077404 and by the Natural Science Foundation of Shanghai under Grant No. 00ZA14078.

References

[1] J. Döring, et al., Z. Phys. A 338 (1991) 457.
[2] G. Winter, et al., Phys. Rev. C 49 (1994) 2427.
[3] J. Döring, et al., Phys. Rev. C 59 (1999) 71.
[4] J.W. Holcomb, et al., Phys. Rev. C 43 (1991) 470.
[5] J. Döring, et al., Phys. Rev. C 47 (1993) 2560.
[6] Q. Pan, et al., Nucl. Phys. A 627 (1997) 334.
[7] A. Harder, et al., Phys. Rev. C 51 (1995) 2932.
[8] R.A. Kaye, et al., Phys. Rev. C 54 (1996) 1038.
[9] K. Hara, et al., Nucl. Phys. A 529 (1991) 445.
[10] K. Hara, et al., Nucl. Phys. A 531 (1991) 221.
[11] K. Hara, et al., Nucl. Phys. A 537 (1992) 77.
[12] K. Hara, et al., Int. J. Mod. Phys. E 4 (1995) 637.
[13] C.G. Andersson, et al., Nucl. Phys. A 309 (1978) 141.
[14] M.A. Rizzutto, et al., Nucl. Phys. A 569 (1994) 547.
[15] A. Bohr, B.R. Mottelson, Nuclear Structure, Vol. 1, Benjamin, Amsterdam, 1969, p. 169.
[16] P. Möller, et al., At. Data Nucl. Data Tables 59 (1995) 185.
[17] J.-Y. Zhang, et al., J. Phys. G 13 (1987) L75.
[18] T. Bengtsson, et al., Nucl. Phys. A 436 (1985) 14.
[19] R. Bengtsson, et al., Phys. Scripta 39 (1989) 196.
[20] G.B. Han, et al., High Energy Phys. Nucl. Phys. 23 (1999) 890 (in Chinese).